Defect identification based on wavelet decomposition for MFL non-destructive inspection of steel plates

D Slesarev

The article considers an application of wavelet decomposition for defect identification based on the example of magnetic flux leakage (MFL) non-destructive testing (NDT). To solve this problem, a parallel signal decomposition is performed for several chosen types of mother wavelet. This article describes the criteria and algorithm for the choice of mother wavelet. A decision tree is used for defect classification. The algorithm presented has been tested both on imitations of defects and on an oil tank floor plate with natural defects.

Keywords: MFL non-destructive testing, defect recognition, wavelet decomposition.

1. Introduction

The solution to many practical problems in non-destructive testing (NDT) is linked with the need to identify defects of several types, which have different hazard rates and differ in their growth rates. This makes it necessary to identify a defect (specify its type) and to estimate its size. Within the magnetic flux leakage (MFL) NDT technique, the solution to this problem has its own specifics and, as such, this technique bears only indirect information about the parameters of a defect. Therefore, the quality of defect parameter estimation depends on the accuracy of the model used to connect the MFL signal with the geometric parameters of the defect. In this regard, for defined defect types the best results can be achieved using methods based on finite element models[1]. However, taking into consideration the full variety of acceptable values of defect parameters, it is difficult to apply finite element models directly to solve the problem of defect detection and identification. It is preferable to solve the detection and identification problem using techniques that allow a set of signals to be described, which correspond to a certain class of defects. This also provides the means to reduce the number of false positives.

One such technique is the wavelet transform. Most frequently, in various NDT methods, a wavelet transform is used to increase the signal-to-noise ratio. It is described in the work by Orth *et al*[2], for example, as improving defect detection at a steel tube mill. Wavelet thresholding is being used for that purpose. Daniel *et al*[3] also describe different wavelet-based denoising techniques for filtering the MFL data to preprocess it for further estimation of defect size by means of an artificial neural network. However, a wavelet transform can be used effectively for signal classification as well. As described in the work by Daniel *et al*[4], for example, discrete wavelet decomposition of Hall-effect sensor signals is used (after the preliminary selection of the area of interest) to classify discontinuities in steam generator tubes. It is of practical significance to consider the possibility of using discrete wavelet decomposition itself to solve the problem regarding the detection and identification of defects, applied directly to measurement signals. This paper presents a solution to this problem. Such processing is simple and offers high-performance as, under certain conditions, it can be reduced to the use of a set of one-dimensional filters and can be used for processing measurement signals in real time, that is,

during testing of an object. This approach may be used not only in magnetic testing but also in other non-destructive testing methods.

MFL testing is widely used for floor inspection of vertical steel storage tanks, as it provides high performance with a reasonable sensitivity to corrosion and does not require the protective coating to be removed[5]. In keeping with contemporary methodology for ensuring the integrity of vertical storage tanks, the MFL technique plays a crucial role in detecting corrosion damage to the tank floor[6].

2. Wavelet decomposition of MFL signals produced by steel plate corrosion

The most common defect types in steel tank floors are the following[7]: dish-shaped general corrosion; pitting corrosion (of the conical profile); and corrosion pipes. Of these, the latter is the most dangerous given its quick development into a hole. The problem of storage tank floor defect classification is considered in[8], in which a statistical classifier based on a modified support vector machine is used to identify the type of corrosion. Implementation of this method requires the use of non-linear programming methods, by which raw measurement data is fed to the classifier input. As demonstrated below, the use of wavelet decomposition can considerably simplify the build-up of the classifier.

The detection of dish-shaped corrosion defects can be quite difficult, as it is characterised by smooth edges. Figures 1(a)-1(c) depict the distribution of the axial component of magnetic leakage field induction over simulations prepared using a steel reference plate for the three types of defect mentioned above: dish-shaped corrosion, 18 mm in diameter and 0.6 T in depth (T is the thickness of the reference plate and in this case it is 6 mm) (Figure 1(a)); imitation of conical-shaped pitting corrosion, 16 mm in diameter and 0.3 T in depth (Figure 1(b)); and imitation of a corrosion pipe, 6 mm in diameter and 0.4 T in depth (Figure 1(c)).

Measurements were made using an Introcor MFL scanner with Hall-effect sensors, arranged in a 150 mm-wide sensor array. While measuring, the scanner is moved above the steel plate. In spite of the greater depth, the signal from the dish-shaped corrosion (Figure 1(a)) is several times weaker than the signal from conical-shaped corrosion (Figure 1(b)). The difference in signal magnitude and signal form is clearly visible. The magnitude is 0.35 mT for 3.6 mm-deep dish-shaped corrosion, 3.5 mT for 1.8 mm-deep pitting corrosion and 2.5 mT for 2.4 mm-deep corrosion pipe. The signal from the corrosion pipe (Figure 1(c)) differs from both of the previous signals; it is more localised in the axial as well as in the transverse direction.
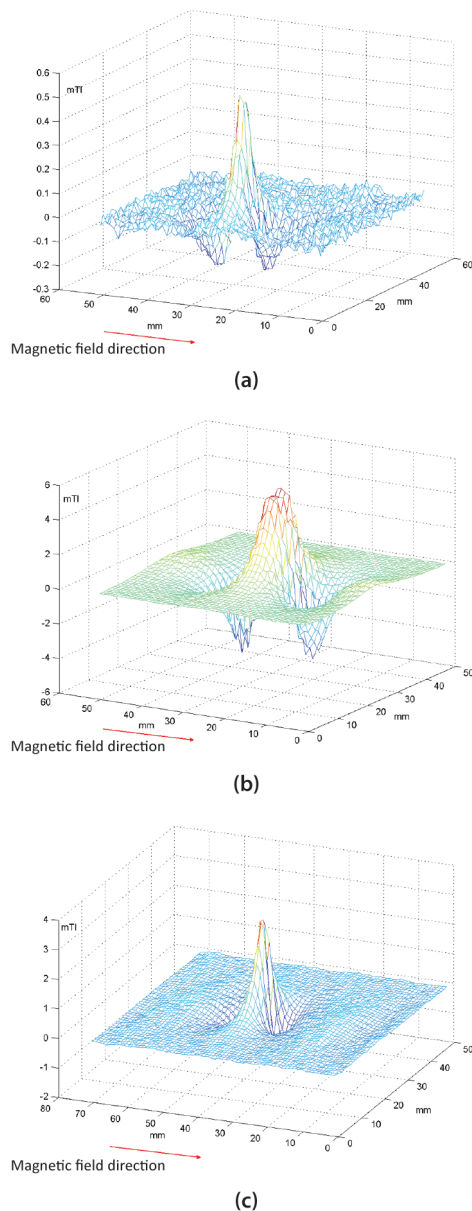

(a)

(b)

(c)

Figure 1. Distribution of the axial component of magnetic leakage field induction over the simulation of: (a) dish-shaped corrosion; (b) pitting corrosion; and (c) corrosion pipe. The red arrows show the direction of the external magnetic field

To apply a wavelet transform for signal processing, basic or mother wavelets should first be selected. In this paper, the author considers the processing of an input signal with a one-dimensional wavelet in the axial direction (which conforms with the scanning direction). Since the problem of defect identification is being dealt with, it is reasonable to choose a different basic wavelet for each type. The selection criteria should be taken as follows: quality of the detection of each type of defect against interference; and quality of the separation of defects among themselves. Additionally, for efficient numerical calculation, basic wavelets should be used that can be realised as digital filters[9]. The formula for the discrete wavelet transform may be written as follows[9]:

$$W_{S,j}(m,n) = 2^{-\frac{m}{2}} \int_{-\infty}^{\infty} S(x) \cdot \psi_j \left(2^{-m}x - n\right) dx \dots\dots\dots (1)$$

where $\psi_j(x)$ is the basic or mother wavelet for the jth type of defect, $S(x)$ is the measured signal, m defines the scale coefficient (2^{-m}) and n is the shift in time or spatial coordinate (and corresponds to t). Using different wavelet decomposition for every defect type, the detection criteria for this defect type may be written as:

$$W_{S,j}(m_j,n) > \Lambda_j \dots\dots\dots\dots\dots\dots\dots\dots (2)$$

where Λ_j is the detection threshold for the jth defect type and m_j is the level of wavelet decomposition that provides the largest portion of energy of the useful signal for a given defect type. For the defect to be best detected, the basic wavelet should derive some typical features of the signal from the corresponding defect[7]. Signal processing is carried out as follows: input signals of every sensor (index k) are processed with selected wavelet filters, on the basis of the Equation (2) two-dimensional map and some areas of interest are formed. For every area of interest, appropriate values $\left\{ \max_{n,k}\left[W_{S_k,j}(m_j,n)\right]\right\}_j$ are acquired for further classification procedures. It is also desirable to calculate wavelet decomposition using a filter with a minimum number of coefficients. A sufficient variety of forms can be achieved using the following: standard Daubechies wavelets of different orders (dbN), symlets of different orders (symN), biorthogonal wavelets (biorN.M) and coiflets (coifN). These wavelets allow for efficient calculation by means of digital filters. Thus, the best wavelets must be chosen from this set. To ensure the detection of all significant corrosion, the signals used to select basic wavelets must conform with signals of the minimal defects of each type (for storage tanks, according to Russian oil & gas industry codes[10], these are defects with a depth of 0.3-0.4 T). It is easier to begin the selection of basic wavelets with the defect type with the strongest signal, since it will create the most false positives when dividing defects into classes. The algorithm for selecting basic wavelets for the case with three types of defect is as follows:

Step 1: Select the basic wavelet ψ_1 and decomposition level m_1, which provide the maximum signal-to-noise ratio (Q) for the signal from a defect of the first type ($S1$):

$$\psi_1, m_1 : \max_{\psi,m}\left\{ Q\left(W_{S1,1}(m_1,n)\right)\right\} \dots\dots\dots\dots (3)$$

where:

$$Q = \frac{\max_n\left\{ W_{S1,1}(m,n)\right\}}{\max_n\left\{ W_{N,1}(m,n)\right\}} \dots\dots\dots\dots\dots (4)$$

N corresponds to the noise at the section of the plate without defect imitation. Normally, this section should be taken as definitely being larger than the size of the largest defect. For the selected ψ_1, m_1, calculate the detection threshold Λ_1 based on the signal from the smallest defect of the first type.

Step 2: Then, select the basic wavelet ψ_2 and decomposition level m_2, such that the appropriate wavelet transform for the signal from a defect of the second type ($S2$) exceeds the ψ_1-wavelet

transform of the same signal with a coefficient β ($\beta > 1$); of the possible options, choose the one with maximum signal-to-noise ratio Q:

$$\psi_2, m_2 : \max_n\{W_{S2,2}(m_2,n)\} > \beta\max_n\{W_{S2,1}(m_1,n)\} \text{ and } \max_{\psi,m}\{Q(W_{S2,2}(m_2,n))\} \ldots (5)$$

For the selected ψ_2, m_2, calculate the detection threshold Λ_2 based on the signal from the smallest defect of the second type.

Step 3: Finally, select the third basic wavelet ψ_3 and decomposition level m_3, such that the appropriate wavelet transform for the signal from a defect of the third type (S3) exceeds both the ψ_1-wavelet transform and ψ_2-wavelet transform of the same signal with a coefficient of β; of the possible options, choose the one with the maximum signal-to-noise ratio Q:

$$\psi_3, m_3 : \max_n\{W_{S3,3}(m_3,n)\} > \beta\max_n\{W_{S3,1}(m_1,n)\}, \max_n\{W_{S3,3}(m_3,n)\} >$$
$$\beta\max_n\{W_{S3,2}(m_2,n)\} \text{ and } \max_{\psi,m}\{Q(W_{S3,3}(m_3,n))\} \ldots (6)$$

For the selected ψ_3, m_3, calculate the detection threshold Λ_3 based on the signal from the smallest defect of the third type.

Steps 2 and 3 are to be iterated: if it is not possible to find a ψ_3 that meets the conditions (Equation(5)), then another ψ_2 is selected and Steps 2 and 3 are repeated. The coefficient β should be chosen from the range from 1 to 2 in order to simplify the selection of the basic wavelets ψ_2 and ψ_3. The method described here has been tested for two reference steel plates with thicknesses of 6 mm and 8 mm and with simulated corrosion of different shapes and sizes (a total of 13 defects). As a result of the algorithm described here, the following basic wavelets and corresponding decomposition levels were selected:

- db2, $m = 2$ for dish-shaped corrosion
- sym6, $m = 3$ for pitting corrosion
- db3, $m = 2$ for corrosion pipe.

Figures 2(a)-2(c) depict the three basic wavelets: db2, sym6 and db3, respectively.

The maximum value of wavelet decomposition calculated for basic wavelets ψ_j that meet the detection criterion (Equation (2)) can be applied as the first classification criterion:

$$j : \max_j\left[\max_{n\in N} W_{S,j}(m_j,n)\right] \ldots (7)$$

where N defines the local area that meets the condition for detection (Equation (2)). In other words, the defect is assigned to the type j that provides the maximum value (Equation(5)).

Verification of the described technique was carried out using a reference plate with three rows of defects, which was scanned using an Introcor scanner, the first row with four imitations of dish-shaped corrosion of different depths (type 1), the second row with five imitations of pitting corrosion of different depths (type 2) and the third row with four imitations of corrosion pipes (type 3). This constitutes a training sample and was used to determine the threshold values of Λ_j. Figure 3 shows a colour diagram (C-scan) of the track of the MFL scanner over the row of pitting corrosion imitations (of conical shape).

Table 1 shows the number of correctly and incorrectly classified defects of each type for the training sample according to the criterion (Equation (5)).
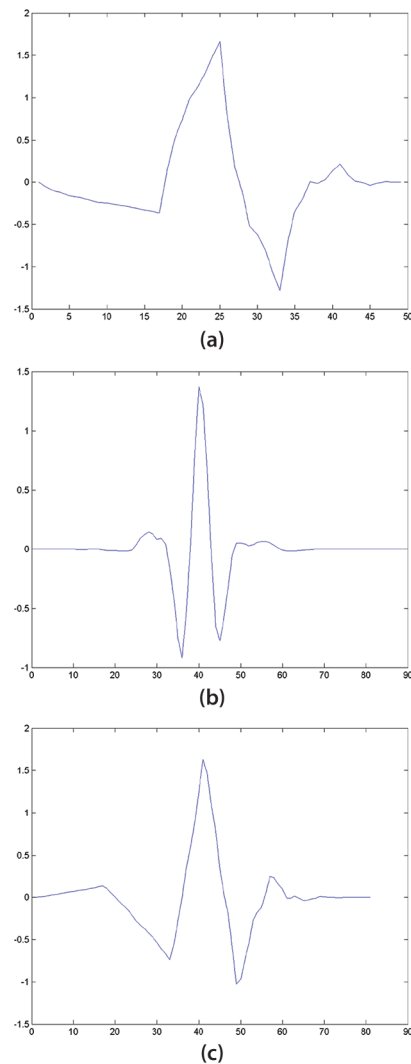

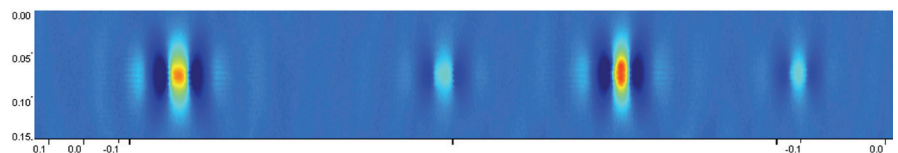**Figure 2.** Basic wavelet for: (a) dish-shaped corrosion, db2; (b) pitting corrosion, sym6; and (c) corrosion pipe, db3

Figure 3. C-scan of the row of pitting corrosion imitations

Table 1. Classification results for the simple threshold algorithm

Type of defect	Number of defects	Maximum value of Equation (5) achieved			Classified correctly
		sym6	db2	db3	
Pitting corrosion	4	4	0	0	4
Dish-shaped corrosion	4	1	2	1	2
Corrosion pipe	5	1	0	4	4

As Table 1 demonstrates, one of the type 2 defects and one of the type 3 defects were mistakenly placed in class 1, and one of the type 2 defects was mistakenly placed in class 3. These mistakes arise for the following reasons: when implementing a processing algorithm based on the comparison of coefficients of the selected wavelet decompositions with preset thresholds, a situation arises where the

signal from a minimal defect, such as pitting corrosion or corrosion pipe, produces a signal that is the same or higher for db2 wavelet coefficient values than for the minimum dish-shaped corrosion (the threshold value for dish-shaped corrosion is nearly ten times lower than for pitting corrosion, due to the low magnitude of the signal). Thus, a simple comparison of the coefficients of three different types of wavelet decomposition $W_{S,j}(m_j, n)$ among themselves is insufficient for correct classification. An additional quantitative feature must be used that reflects the relationship of the decomposition coefficients of different basic wavelets to the signals of defects of the same class. Below, the author introduces such an additional feature and describes the construction of a decision tree that takes this feature into account and improves the reliability of defect classification. As such an additional feature, the author uses the ratio of the maximum wavelet coefficient of the investigated signal with a basic wavelet of presumptive class to the maximum wavelet coefficients of the investigated signal with basic wavelets of alternative classes:

$$\max_n \left\{ W_{S,i}(m_i, n) \right\} \Big/ \max_n \left\{ W_{S,j}(m_j, n) \right\}, \quad i \neq j \ldots\ldots\ldots (8)$$

This ratio is compared with the constants σ_1, σ_2 and σ_3, which are determined during the training process of the classification algorithm by averaging over all defects of the training sample. For example, to identify a signal as being due to dish-shaped corrosion, it is proven that the maximum of its db2 decomposition coefficients $\max\{W_{S,1}(m_1)\}$ exceeds the corresponding threshold Λ_1 (this value is rather low because of the low magnitude of dish-shaped corrosion signals). To exclude pitting and pipe-type corrosion (the signals of which are greater than the signals of dish-shaped corrosion), the relationship of $\max\{W_{S,2}(m_2)\}$ to $\max\{W_{S,1}(m_1)\}$ and the relationship of $\max\{W_{S,3}(m_3)\}$ to $\max\{W_{S,1}(m_1)\}$ are proven, which should not exceed appropriate values of σ_1 and σ_2.

Generally, the classification procedure is built as a decision tree based on the classification and regression tree (CART) algorithm[11]. In the nodes of the tree, the conditions for movement are formulated to a further node or final classification, a leaf based on comparison of the maximum values of the wavelet coefficients (Equation (7)) with the corresponding threshold values as well as with each other. The decision tree is depicted in Figure 4. To increase the stability of the training result, signals from interference recorded while scanning a real tank floor were added to the training sample in addition to signals from reference defects.
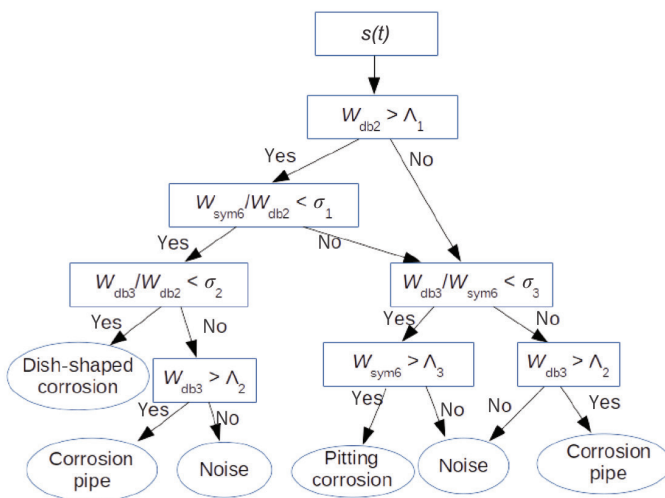
The constants σ_j are defined so as to minimise the probability of false classification, calculated as the frequency of incorrect judgements. The training process of the algorithm, using the sample described above, allowed the following coefficients to be obtained: $\sigma_1 = 1.28$, $\sigma_2 = 1.05$ and $\sigma_3 = 1.95$. Application of the decision tree to the training sample provided error-free classification of the defects. Taking into account the size of the training sample, the numerical values of the coefficients are determined with 90% classification confidence. Application of the decision tree classification algorithm to the same training sample as before resulted in 100% correct classification (all 13 defects were classified correctly).

Inspection data of a real tank floor plate of 6 mm thickness made by the Introcor scanner, including eight tracks, was used to test the proposed algorithm. A C-scan of one of the tracks is shown in Figure 5. 51 defects that exceeded the detection threshold were detected on the plate. The detected defects were confirmed by visual and instrumental methods. The results are shown in Table 2. Some of the assumed fault zones corresponded with interference. In total, 43 of 51 defects were correctly classified and ten false zones were also identified (false calls). Overall, the procedure achieves an 84% correct classification; however, the number of dish-shaped corrosion defects is too few correct statistical observation (because of low signal magnitude, the risk of incorrect classification of this type of defect is higher than for other types).
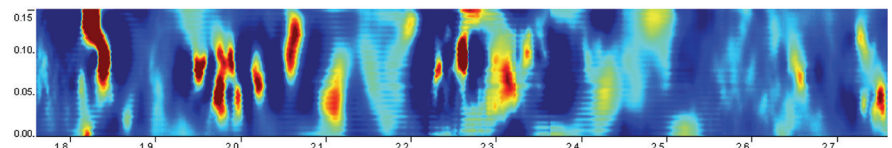

Figure 5. C-scan of one of the tracks above the tank floor plate with multiple corrosion defects

Table 2. Results of defect classification for the tank floor plate with real corrosion

Type of defect	Number of defects	Correctly classified	Fault zones
Pitting corrosion	34	30	2
Dish-shaped corrosion	6	3	4
Corrosion pipe	11	10	4

False zones may be filtered out in part by additional processing of data in the transverse direction, but this research did not directly deal with this task.

3. Conclusion

The challenge of defect identification in MFL non-destructive testing can be addressed by means of highly efficient parallel wavelet decomposition of the investigated signal with several types of basic wavelet, which should be selected optimally. To increase classification confidence, the relationship between the decomposition coefficients of the investigated signal with different basic wavelets is used as an additional criterion. Defect identification can be implemented effectively using a recognition algorithm

Figure 4. Decision tree for corrosion classification

based on a decision tree. At the sample plate from the real tank floor with 51 corrosion defects, the proposed algorithm has shown 84% classification confidence.

References

1. V Lunin and D Alexeevsky, 'Numerical prediction of signal for magnetic flux leakage benchmark task', Review of Progress in Quantitative Nondestructive Evaluation, Vol 22, pp 1830-1837, 2003.

2. T Orth, T Schmitte, R Peters, K-D Müller, A Koka and S Nitsche, 'Wavelet signal processing of magnetic flux leakage signals – implementation of a multi-channel wavelet filter for non-destructive testing systems in steel tube mills', Proceedings of the Sixth International Workshop on Advances in Signal Processing for Non Destructive Evaluation of Materials, London, Ontario, Canada, 24-27 August 2009.

3. J Daniel, R Mohanagayathriand and A Abudhahir, 'Characterisation of defects in magnetic flux leakage (MFL) images using wavelet transform and neural network', Proceedings of the 2014 International Conference on Electronics and Communication Systems (ICECS), Coimbatore, India, 13-14 February 2014.

4. J Daniel, A Abudhahir, K Shankar and S Pandi, 'Detection and classification of discontinuities using discrete wavelet transform and MFL testing', Materials Evaluation, Vol 76, No 6, pp 706-715, 2018.

5. D Slesarev and A Abakumov, 'Data processing and presentation in MFL technique of non-destructive testing', Russian Journal of Nondestructive Testing, Vol 49, No 9, pp 493-498, 2013.

6. D Papasalouros, K Bollas, D Kourousis, N Tsopelas and A Anastasopoulos, 'Modern inspection methodologies for RBI programs of atmospheric storage tanks', 11th European Conference on Non-Destructive Testing (ECNDT 2014), Prague, Czech Republic, 6-10 October 2014.

7. Mitsui Babcock Energy Limited, 'HSE RR481: Recommended practice for magnetic flux leakage inspection of atmospheric storage tank floors', 2006.

8. A R Ramirez, N Pearson and J Mason, 'A holistic approach to automatic classification of steel plate corrosion defects using magnetic flux leakage', 17th World Conference on Non-Destructive Testing (WCNDT 2008), Shanghai, China, 25-28 October 2008.

9. I Daubechies, Ten Lectures on Wavelets, Philadelphia, USA, 1995.

10. Gosgortekhnadzor of Russia, 'RD 08-95-95 Provision on the system for technical diagnostics of welded vertical cylindrical oil and petroleum products tanks', 1995.

11. L Breiman, J H Friedman, R A Olshen and C T Stone, Classification and Regression Trees, Wadsworth, Belmont, California, USA, 1984.